NIH Public Access
Author Manuscript
Circ Res. Author manuscript; available in PMC 2013 August 26.

Published in final edited form as:
Circ Res. 2003 May 2; 92(8): 920–928. doi:10.1161/01.RES.0000069030.30886.8F.

Increased Fibronectin Deposition in Embryonic Hearts of Retinol-Binding Protein–Null Mice

Christopher C. Wendler, **Angela Schmoldt**, **George R. Flentke**, **Lauren C. Case**, **Loredana Quadro**, **William S. Blaner**, **John Lough**, and **Susan M. Smith**
Department of Cell Biology, Neurobiology, and Anatomy and the Cardiovascular Center (C.C.W., A.S., L.C.C., J.L.), Medical College of Wisconsin, Milwaukee; the Department of Nutritional Sciences (G.R.F., S.M.S.), University of Wisconsin-Madison; the Department of Medicine (W.S.B.), Columbia University College of Physicians and Surgeons, New York, NY; Institute of Cancer Research (L.Q.), Columbia University College of Physician and Surgeons, New York, NY; and the Department of Biological and Environmental Sciences (L.Q.), University of Sannio, Benevento, Italy.

Abstract

Precise regulation of retinoid levels is critical for normal heart development. Retinol-binding protein (RBP), an extracellular retinol transporter, is strongly secreted by cardiogenic endoderm. This study addresses whether RBP gene ablation affects heart development. Despite exhibiting an >85% decrease in serum retinol, adult RBP-null mice are viable, breed, and have normal vision when maintained on a vitamin A-sufficient diet. Comparison of RBP-null with wild-type (WT) hearts from embryos at day 9.0 (E9.0) through E12.5 revealed an RBP-null phenotype similar to that of other retinoid-deficient models. At an early stage, RBP-null hearts display retarded trabecular development, which recovers by E9.5. This is accompanied at E9.5 and E10.5 by precocious differentiation of subepicardial cardiac myocytes. Most remarkably, RBP-null hearts display augmented deposition of fibronectin protein in the cardiac jelly at E9.0 through E10.5 and in the outflow tract at E12.5. This phenomenon, which was detected by immunohistochemistry and Western blotting without increased fibronectin transcript levels, is accompanied by increased numbers of mesenchymal cells in the outflow tract but not in the atrioventricular canal. RBP-null cardiac myocytes, especially in the subepicardial layer, display increased cell proliferation. This phenotype may present a model of subclinical retinoid insufficiency characterized by alteration of an extracellular matrix component and altered cellular differentiation and proliferation, changes that may have functional consequences for adult cardiac function. This murine model may have relevance to fetal development in human populations with inadequate retinoid intake.

Keywords

retinol-binding protein knockout; retinoic acid; mouse heart development; cardiac jelly; fibronectin

The biologically active derivative of vitamin A, retinoic acid (RA), plays an essential role in regulating the homeostasis of adult organs as well as the development of numerous embryonic tissues. Precisely regulated retinoid levels are crucial for normal development of the cardiovascular system: too much or too little RA causes profound cardiac

© 2003 American Heart Association, Inc.

Correspondence to: Dr John W. Lough, Department of Cell Biology, Neurobiology and Anatomy, Medical College of Wisconsin, 8701 Watertown Plank Rd, Milwaukee, WI 53226. jlough@mcw.edu.

NIH-PA Author Manuscript
NIH-PA Author Manuscript
NIH-PA Author Manuscript

NIH-PA Author Manuscript

NIH-PA Author Manuscript

NIH-PA Author Manuscript

teratogenicity.[1,2] For example, excess RA causes effects ranging from diminished cardiac jelly and outflow tract (OFT) disruption[3,4] to the total and specific absence of the embryonic heart.[5] On the other hand, vitamin A deficiency (VAD) causes aortic arch anomalies, ventricular septal defects, and retarded myocardial development[6] reflecting cellular deficits, including hypoplastic myocardial walls that contain precociously differentiated cardiac myocytes.[7,8] Most deficits caused by VAD are recapitulated by ablation of the genes involved in retinoid synthesis, such as retinaldehydeoxidizing dehydrogenase (RALDH2),[9] or genes in the retinoid signaling pathway, including the RA receptor (RAR) and retinoid X receptor (RXR) genes.[7,8,10,11] These findings suggest that the ablation of genes that regulate retinoid delivery, such as the retinol-binding protein (RBP) gene, may adversely affect heart development.

Interest in this possibility was prompted by findings that definitive endoderm, which is indispensable for the differentiation of precardiac mesoderm,[12] robustly secretes RBP[13] while comigrating with precardiac mesoderm during gastrulation. On appearance of the definitive heart, RBP and its adult binding partner, transthyretin, are respectively localized in myocytes and in the cardiac jelly, with the latter being a shared basement membrane manufactured by surrounding endocardial and myocardial cells. Thus, the development of a retinoid-sensitive organ such as the heart may depend on a regulated sequence of retinoid delivery that begins with the transport of vitamin A by RBP. To investigate this possibility we have examined heart development in RBP-null mice. Although RBP-null adults are viable and fertile, they cannot mobilize vitamin A stores, inasmuch as they exhibit levels of circulating retinol that are up to 90% below normal[14]; hence, these mice constitute a model for subclinical VAD. We report that although RBP-null embryos do not show profound VAD symptoms, they do exhibit phenotypic traits consistent with retinoid deficiency. These include (1) most remarkably, increased deposition of fibronectin (Fn) in cardiac jelly and nascent valves concomitant with (2) retarded trabecular development, (3) increased cell numbers in OFT endocardial cushion, (4) increased myocyte proliferation, and (5) precocious differentiation of myocytes in the compact layer of myocardium.

Materials and Methods

Production and Immunohistochemical Processing of RBP-Null Mouse Embryos

RBP mutant mice were prepared by Quadro et al.[14] RBP-null and control wild-type (WT) mice were maintained on a mixed genetic background (129/Sv, C57BL/6, CD-1), predominantly C57BL/6. Mice were fed ad libitum rodent chow (Purina No. 5010) containing 44 IU vitamin A (acetate) per gram diet and 4.5 ppm carotene. Embryos were staged by enumerating somite pairs, immediately fixed by cryopreservation, embedded in paraffin, and sectioned. For immunohistochemical analysis, primary antibodies included rabbit anti-Fn and mouse anti–α-sarcomeric actin, the secondary antibodies for which were fluorescein goat anti-rabbit IgG or goat anti-mouse IgM, respectively. Nuclei were stained with DAPI or propidium iodide (PI).

Digital Image Analysis and Electron Microscopy

The cardiac phenotypes of three pairs of somite-matched WT and RBP-null embryos at day 9.5 (E9.5) were evaluated via quantitative morphometry of heart sections immunostained for α-sarcomeric actin. Electron microscopy was performed on three pairs of WT and RBP-null hearts from E9.5 and E10.5 embryos. The cellular ultra-structure in each heart was evaluated with the investigator blinded to the experimental conditions. Statistical significance was determined via SE and *t* test analyses.

NIH-PA Author Manuscript

NIH-PA Author Manuscript

NIH-PA Author Manuscript

Cell Proliferation

5′-Bromo-2′-deoxyuridine (BrdU) was injected at 0.1 mg/g body wt into the peritoneal cavity of pregnant mice at 10.5 postcoital days; 4 hours later, embryos were processed for enumeration of BrdU-substituted nuclei on a background of PI-stained nuclei. Total myocardial, trabecular, and subepicardial myocyte subsets were evaluated, in a blinded fashion, in 5 hearts each from WT and RBP-null embryos.

Western Blotting

Whole intact embryonic hearts or livers were dissolved in electrophoresis buffer, and proteins were electrophoretically separated and blotted onto nitrocellulose, followed by detection of Fn using successive application of anti-Fn antibody, goat anti-rabbit IgG–horseradish peroxidase antibody, and an enzyme-linked chemiluminescence reagent. Quantitative digital processing of Fn images was used to calculate the increase of Fn in RBP-null tissues.

Northern Hybridization and Real-Time Polymerase Chain Reaction

Total RNA was purified from embryonic hearts, followed by separation of 1 μg in each lane of a 1% agarose/formaldehyde gel. Blots were hybridized with an antisense riboprobe complementary to mouse Fn cDNA.

In Situ Hybridization

Transcripts encoding RBP and Fn were detected in embryonic sections as previously described,[15] except that proteinase K digestion time was only 3 minutes. The Fn antisense riboprobe was identical to that used for Northern analysis; the RBP antisense riboprobe was full-length and was transcribed from IMAGE clone No. 303723.After development, the sections were counterstained with PI and photographed.

An expanded Materials and Methods section can be found in the online data supplement available at http://www.circresaha.org.

Results

RBP Expression in Early Embryogenesis

To facilitate interpretation of the RBP-null phenotype, a detailed analysis of RBP expression was performed by in situ hybridization on WT embryos. At E7.5 (Figure 1A), transcripts were enriched in the visceral endoderm, the site of retinol transfer from maternal tissues (RBP does not cross the placenta); expression in the visceral endoderm was detected at the blastocyst stage (not shown). By 22 somites (E9.5), transcripts within the embryo itself were most abundant in the gut endoderm (Figure 1B). This expression intensified at E10.5 (Figure 1C); by E11.5, the liver was the dominant site of RBP expression (Figure 1D), with transcripts barely detected in the hindgut endoderm (Figure 1D). Surprisingly, strong RBP expression was seen in the pancreatic rudiment (Figure 1D) and at lower but clearly identifiable levels along the notochord (Figure 1E). Although the early heart is enriched in RBP protein,[13] at no time were RBP transcripts detected in cardiomyocytes or endocardiocytes. Hence, RBP that is localized in the early cardiac jelly must have originated from extracardiac sources, presumably the liver and gut endoderm.

RBP-Null Mice Reveal No Overt Dysmorphology

Neither RBP-null embryos nor whole hearts exhibited gross anatomic anomalies (see online Figure 1, available at http://www.circresaha.org) other than slightly diminished overall size, which was a subtle albeit consistent observation. No instances of cardia bifida or atrial

NIH-PA Author Manuscript

NIH-PA Author Manuscript

NIH-PA Author Manuscript

expansion indicative of high retinoid levels[16] were observed, nor were VAD symptoms, such as sinus venosus obliteration.[17] Rightward looping of the cardiac tube, which is randomized during retinoid excess or absence,[9,18] was also normal. Chamber identity was normal at all stages up to E12.5, as indicated by the expression of ventricular (MLC-2v) and atrial (MLC-2a) markers (not shown).

RBP-Null Mice Display Elevated Fn Deposition in Cardiac Jelly

Prompted by findings that retinoid levels affect Fn expression,[4,19] hearts from somite-matched embryo pairs between E9.0 and E12.5 were evaluated for Fn deposition using immunohistochemistry. Figure 2 shows that Fn deposition in cardiac jelly of RBP-null hearts was in significant excess. Although Fn expression by myocardial cells is normally attenuated at later stages,[20] Fn deposition in RBP-null hearts becomes most pronounced at E12.5 (Figure 3), particularly in valves of the OFT (Figures 3B and 3E) and atrioventricular (AV) canal (Figure 3B). Regarding littermates, WT and heterozygous embryos exhibited low Fn levels that were indistinguishable (Figures 3C and 3D) in contrast with RBP-null littermates (Figure 3E). This phenomenon was observed in all basal laminae of RBP-null embryos.

Fn Gene Transcription Is Unaffected in RBP-Null Hearts

To assess whether the increase in Fn protein was correlated with increased transcript levels, Northern and in situ hybridization analyses were performed. Northern blotting (Figure 4) demonstrated that although Fn transcripts were enriched in the heart relative to the whole embryo at E10.5, transcript levels in WT and RBP-null samples were similar. This observation was corroborated by real-time polymerase chain reaction of RBP-null hearts (not shown). In situ hybridization revealed that Fn transcript distribution was similar in WT and RBP-null embryos (Figure 5), with most cardiac transcripts in epicardial and endocardial cells (arrowheads, Figures 5A through 5D) and in cushion mesenchyme (arrows, Figures 5G and 5H); Fn transcripts were notably absent in the myocardium. Finally, Fn expression in the liver, a major source of circulating Fn protein, was unchanged in RBP-null embryos (Figures 5E and 5F).

Fn Protein Is Increased in RBP-Null Hearts

Results in Figures 4 and 5 indicate that increased deposition of Fn protein in cardiac jelly of RBP-null hearts was not caused by increased Fn gene transcription. Hence, the immunostaining pattern in Figures 2 and 3 was corroborated by Western blotting, revealing that Fn protein content was increased in RBP-null tissues. As shown in Figure 6A, blots containing identical protein fractions from RBP-null/WT tissue pairs revealed increasing Fn levels in RBP-null hearts between E9.0 and E12.5. Figure 6B shows similar data from E9.0 through E9.5 hearts staged according to somite pairs, indicating that Fn increase in RBP-null hearts at these early stages was approximately linear. Panel C in Figure 6 shows typical Western blots that were used to construct the data in panels A and B. The data in Figures 4 through 6 indicate that increased Fn protein in RBP-null embryos was caused by altered synthesis and/or degradation of Fn protein.

Cytoarchitecture in RBP-Null Hearts

The above findings, plus the cellular consequences of retinoid deficiency,[7–9] prompted the evaluation of trabeculation and myocardial wall thickness. Trabecular development was 50% reduced in E9.0 RBP-null embryos containing 18 somite pairs; however, this deficit was transient and was not observed in embryos containing 24 (E9.5) or 36 (E10.5) somite pairs (online Figure 2). Ventricular wall thickness was calculated from its circumscribed area, as determined by analysis of tissue immunostained with antisarcomeric α-actin

NIH-PA Author Manuscript

NIH-PA Author Manuscript

NIH-PA Author Manuscript

(MetaMorph Imaging System, Universal Imaging Corporation). These measurements, which were made on serial sections through the entirety of three WT and RBP-null E9.5 hearts, detected no significant differences in myocardial wall volume (WT 7.2×10^5 μm^3, null 7.2×10^5 μm^3); similarly, the calculation of whole luminal areas (not shown) and volumes occupied by hearts (WT 1.4×10^6 μm^3, null 1.4×10^6 μm^3) revealed no differences. Finally, considering the possible relationship between Fn deposition and cellular migration during the epithelial-mesenchymal transition that initiates AV and OFT cushion formation, cell numbers in endocardial cushions were enumerated at E9.5, revealing significantly increased mesenchymal cell numbers in the OFT cushion of RBP-null hearts (online Figure 3).

Cardiac Myocyte Proliferation Is Increased in RBP-Null Embryos

To ascertain whether increased Fn deposition was associated with cell proliferation, the numbers of myocardial cells in cell-cycle transit within E10.5 hearts were enumerated by BrdU incorporation. Cells constituting the entire myocardium, as well as cells restricted to subepicardial (compact) and trabecular areas, were evaluated (Figure 7). Considering the entire myocardium, 29% of WT myocytes incorporated BrdU, compared with 38% of RBP-null myocytes. Analysis of the trabecular myocyte subset revealed a similar increase, from 30% in WT myocytes to 42% in RBP-null myocytes. Most remarkably, the proliferation rate in subepicardial myocytes increased from 32% in WT hearts to 49% in RBP-null hearts.

Differentiation of Subepicardial Myocytes Is Increased in RBP-Null Embryos

Ablation of genes in the retinoid-signaling pathway causes precocious differentiation of myocytes in the subepicardial layer of myocardium.[8] Hence, we compared cytodifferentiation of myocytes in WT and RBP-null hearts. Figure 8 shows electron micrographic data from E9.5 and E10.5 myocytes in which the extent of differentiation was estimated by enumerating Z disks, precursors of sarcomeres. Randomly located myocytes within the entire myocardium and myocytes restricted to the subepicardial layer were separately evaluated using a magnification of ×8000. Considering the entire myocardium, the numbers of Z disks per myocyte did not differ in WT and RBP-null hearts (not shown). However, myocytes in the subepicardium of RBP-null hearts at E9.5 revealed precociously high numbers of Z disks (defined as >4, Figure 8C), a trend that persisted at E10.5 (Figure 8D).

Discussion

Transthyretin and RBP are perhaps the major products of embryonic endoderm,[13] the secretions from which enable precardiac mesoderm to attain its fully differentiated state.[12] Shortly after the definitive heart appears, RBP protein, initially of endoderm and later of liver origin, is detected in the cardiac jelly.[13] Considering the adult role of RBP as a retinol carrier protein, as well as the need for precisely regulated retinoid levels during early heart development, we found it of interest to examine the effect of RBP ablation on cardiogenesis. The potential importance of RBP was suggested by its early and continuous expression during embryogenesis[13,21] and by evidence that suppression of RBP disrupts the development of vitelline vessels and neural structures.[22] The severe photoreceptor defects caused by ablation of the interphotoreceptor RBP (IRBP) gene[23] are also relevant, inasmuch as IRBP is an extracellular protein that transfers retinoids between cells of the retina. Although IRBP is structurally unrelated to RBP, their functional homology suggests roles in regulating retinoid levels in avascular areas, such as the extracellular matrices of the retina (IRBP) and heart (RBP, cardiac jelly). These findings suggest that RBP ablation could cause cardiac developmental defects that are perhaps due to retinoid insufficiency or to an unknown contribution of RBP protein to embryogenic processes.

NIH-PA Author Manuscript

NIH-PA Author Manuscript

NIH-PA Author Manuscript

The RBP-null phenotype included transiently impaired trabeculation and precociously developed subepicardial myocytes. These defects resemble a mild version of the heart phenotype seen in retinoid receptor–null (RXRα, RXRβ, and RARα)[7,8,10,11] and RALDH2-null[9] mice, with the latter being a major RA synthetic enzyme. Hence, RBP ablation causes developmental deficits in the spectrum of retinoid deficiency. The failure of RBP ablation to recapitulate severe VAD phenotypes[2,6] may reflect compensation by dietary retinoids, even though circulating retinol levels in these mice are only 10% to 20% of normal values.[14] Although the reduction of vitamin A to these levels does not cause frank deficiency symptoms such as inanition or motor weakness, such levels cause disorders including immunosuppression[24] and impaired visual acuity.[14] This raises clinically relevant concerns. For example, low levels of vitamin A remain common in population segments of both developed[25] and underdeveloped[26] nations. Although the aberrations reported in the present study are of uncertain consequence, echocardiography and direct examination of adult RBP-null mice revealed significant heart enlargement accompanied by increased left ventricular wall thickness (authors' unpublished data, 2003). Therefore, it is of concern that similar levels of retinoid insufficiency during human pregnancy could expose offspring to unknown cardiovascular risk.

In addition to the mild VAD phenotype, RBP-null embryos exhibited increased endocardial cushion cell numbers, myocyte proliferation, and, most remarkably, deposition of Fn in cardiac jelly and nascent valves. This latter observation is consistent with the positive regulation of Fn reported for VAD hepatocytes[19,27] and perhaps also with the enlarged cardiac jelly space observed in RALDH2-null hearts,[9] although this matrix was not examined. It also is consistent with the reduced Fn deposition in the cardiac jelly of embryos treated with RA.[3,4] Data in Figures 4 through 6 indicate that increased Fn deposition likely results from misregulated protein synthesis and/or matrix degradation, although subtle changes in Fn mRNA levels could contribute to the accumulation. Regarding the latter, a canonical retinoic acid response element (RARE) has not been described in the Fn promoter,[28] and whereas some studies have reported transcriptional upregulation of Fn under VAD conditions,[19] others have shown that RA negatively regulates Fn at the translational level.[28] It is of interest that Fn expression in adult myocytes and cardiac fibroblasts is strongly regulated by cytokines.[29,30] Hence, we are investigating the Fn phenotype in RBP-null embryos using a microarray approach to identify (1) matrix components that may be misregulated and (2) possible roles for extracellular proteases and protease inhibitors.

During heart development, Fn substrates are required to support the migration of precardiac mesoderm during gastrulation[31,32] and mesenchymal cells during cushion formation.[33] Curiously, in situ hybridization (Figure 5) has suggested that cardiac jelly Fn is strongly expressed by endocardial cells with virtually no contribution from the myocardium; because Fn is expressed by early myocardial cells in chick embryos,[20] hybridization at earlier stages in mouse development will clarify this issue. Considering the amount of cardiac jelly Fn in RBP-null mice, it was not surprising that mesenchymal cell numbers were increased in the developing OFT cushion. That this phenomenon was less pronounced in the AV cushion is consistent with observations that RA treatment reduces Fn in the OFT cushion only.[3] Moreover, high RA levels decrease mesenchymal cell numbers in AV and OFT cushions.[3] To our knowledge, mesenchymal cell numbers in OFT cushions have not been monitored in VAD models before E12.5, when RXRα/RARβ double-knockout[34] and RXRα knockout[35] mice exhibit increased OFT mesenchymal cell apoptosis. The latter may be reconciled with our observation of increased mesenchymal cells in the OFT of RBP-null hearts by considering that VAD causes an increased migration of cushion cells at early stages that may be overcompensated later by abnormally increased apoptosis.

NIH-PA Author Manuscript

NIH-PA Author Manuscript

NIH-PA Author Manuscript

Precocious differentiation and mitotic indices of subepicardial myocytes are decreased in retinoid receptor–null hearts.[8] Although RBP-null hearts contained precociously differentiated subepicardial myocytes (Figure 8), this was accompanied by an increased myocyte proliferation (Figure 7) that was particularly remarkable in the subepicardial subset. This difference is difficult to reconcile. Possibly, these data reflect different roles for RBP and retinoid receptors during myocyte proliferation, or these data may reflect differences in how myocyte proliferation was evaluated; specifically, whereas mitotic indices are relatively difficult to discern and are present in low numbers, BrdU-labeled nuclei are prominent and present in relatively high numbers. Surprisingly, whether the quantity or quality of Fn substrate affects the proliferation of embryonic myocytes has not been addressed, although increased Fn is positively correlated with the proliferation of adult cardiac fibroblasts.[36] More pertinently, Fn production by fetal myocytes is positively correlated with their proliferation, and whereas inhibition of integrin $\alpha_5\beta_1$, a Fn receptor, suppressed myocyte proliferation, stimulation of integrin $\alpha_5\beta_1$ induced proliferation.[37] Although the Fn global knockout is of limited value in interpreting the RBP-null phenotype because of its early embryonic lethality, it is curious that this phenotype appears to have a cardiovascular origin.[38] The interesting question of whether regulated deposition of Fn in the embryonic heart is required for normal myocyte proliferation could be examined in mice carrying either conditionally targeted Fn alleles and/or Fn transgenes under the control of a myocardium-specific promoter.

Another feature of the RBP ablation was transiently inhibited trabeculation. More pronounced disruption of trabeculation has been observed in retinoid receptor–null and RALDH2-null mutants.[8–11] It is speculated that reduced trabeculation is due to defective cell-cell adhesion, inasmuch as RALDH2 mutants display a nonintegrated myocardium[9]; however, this is not observed in the RBP-null phenotype. It could be considered that disrupted trabeculation in these models and during VAD[6] is related to Fn overabundance, which could be investigated in a transgenic model of myocardium-specific Fn overexpression. Coincidentally, the recovery of trabecular formation at E9.5 coincides with the establishment of the embryonic circulation, suggesting rescue by retinoids from non–RBP-dependent sources such as serum lipoproteins; although the epicardium may supply the outer heart wall with RA,[39] trabeculation in RBP-null mice is restored at E9.5, before epicardial formation.

Although RBP-null hearts exhibit molecular and cellular alterations that may affect cardiac function in a subclinical fashion, they exhibit no detectable gross dysmorphology. This relatively modest phenotype, in contrast with other retinoid knockouts, is likely explained by the contribution of retinoids from dietary sources. Because dietary retinoids may have obscured penetrance of the RBP-null phenotype, we are examining the effect of RBP ablation in embryos from which dietary retinoids are precipitously withdrawn at specific cardiogenic stages. Because this should render developing embryos virtually retinoid null, knowledge concerning the effect of retinoid levels on the development of the cardiovascular as well as other organ systems should be extended.

Finally, RBP-null mice may be useful in investigating unsuspected roles of RBP in the embryo. For example, this is the first report of RBP transcripts in the notochord (Figure 1), an interesting observation considering that the adjacent floor plate is a source of RA.[40] RBP is also expressed by the pancreatic rudiment, and during the development of this pancreatic rudiment, RA enhances duct morphogenesis while suppressing acinar differentiation via induction of laminin-β1, a modulator of ductal differentiation.[41] It is curious that RBP expression in the E11.5 pancreas occurs concomitantly with the respective epithelial and mesenchymal expression of RALDH2 and RARα in this organ, coinciding with their

NIH-PA Author Manuscript

NIH-PA Author Manuscript

NIH-PA Author Manuscript

regulation of matrix signals that influence exocrine differentiation. Whether RBP contributes to these developmental processes merits further investigation.

Supplementary Material

Refer to Web version on PubMed Central for supplementary material.

Acknowledgments

This study was supported by NIH grants F32-HL-67561 (Dr Wendler), R01-HL-61911 (Drs Lough and Smith), R01-DK-52444 (Dr Blaner), R01-EY-12858 (Dr Blaner), and P01-ES-09090 (Dr Smith) and Hatch Award No. 3863 (Dr Smith). We thank Mei Baker for performing the real-time polymerase chain reaction.

References

1. Zile MH. Function of vitamin A in vertebrate embryonic development. J Nutr. 2001; 131:705–708. [PubMed: 11238746]
2. Smith S, Dickman E. New insights into retinoid signaling in cardiac development and physiology. Trends Cardiovasc Med. 1997; 7:53–58.
3. Nakajima Y, Morishima M, Nakazawa M, Momma K. Inhibition of outflow cushion mesenchyme formation in retinoic acid-induced complete transposition of the great arteries. Cardiovasc Res. 1996; 31:77–85.
4. Nakajima Y, Morishima M, Nakazawa M, Momma K, Nakamura H. Distribution of fibronectin, type I collagen, type IV collagen, and laminin in the cardiac jelly of the mouse embryonic heart with retinoic acid-induced complete transposition of the great arteries. Anat Rec. 1997; 249:478–485. [PubMed: 9415455]
5. Drysdale TA, Patterson KD, Saha M, Krieg PA. Retinoic acid can block differentiation of the myocardium after heart specification. Dev Biol. 1997; 188:205–215. [PubMed: 9268569]
6. Wilson JG, Warkany J. Aortic-arch and cardiac anomalies in the offspring of vitamin A deficient rats. Am J Anat. 1949; 85:113–155. [PubMed: 18138113]
7. Kastner P, Grondona JM, Mark M, Gansmuller A, LeMeur M, Decimo D, Vonesch J-L, Dolle P, Chambon P. Genetic analysis of RXRα development function: convergence of RXR and RAR signaling pathways in heart and eye morphogenesis. Cell. 1994; 78:987–1003. [PubMed: 7923367]
8. Kastner P, Messaddeq N, Mark M, Wendling O, Grondona JM, Ward S, Ghyselinck N, Chambon P. Vitamin A deficiency and mutations of RXRα, RXRβ, and RAR-α lead to early differentiation of embryonic ventricular cardiomyocytes. Development. 1997; 124:4749–4758. [PubMed: 9428411]
9. Niederreither K, Vermot J, Messaddeq N, Schuhbaur B, Chambon P, Dolle P. Embryonic retinoic acid synthesis is essential for heart morphogenesis in the mouse. Development. 2001; 128:1019–1031. [PubMed: 11245568]
10. Gruber PJ, Kubalak SW, Pexieder T, Sucov HM, Evans RM, Chien KR. RXRα deficiency confers genetic susceptibility for aortic sac, conotruncal, atrioventricular cushion, and ventricular muscle defects in mice. J Clin Invest. 1996; 98:1332–1343. [PubMed: 8823298]
11. Mendelsohn C, Lohnes D, Decimo D, Lufkin T, LeMeur M, Chambon P, Mark M. Function of the retinoic acid receptors (RARs) during development, II: multiple abnormalities at various stages of organogenesis in RAR double mutants. Development. 1994; 120:2749–2771. [PubMed: 7607068]
12. Lough J, Sugi Y. Endoderm and heart development. Dev Dyn. 2000; 217:327–342. [PubMed: 10767078]
13. Barron M, McAllister D, Smith SM, Lough J. Expression of retinol binding protein and transthyretin during early embryogenesis. Dev Dyn. 1998; 212:413–422. [PubMed: 9671945]
14. Quadro L, Blaner WS, Salchow DJ, Vogel S, Piantedosi R, Gouras P, Freeman S, Cosma MP, Colantuoni V, Gottesman ME. Impaired retinal function and vitamin A availability in mice lacking retinol-binding protein. EMBO J. 1999; 18:4633–4644. [PubMed: 10469643]
15. Power SC, Lancman J, Smith SM. Retinoic acid is essential for Shh/Hoxd signaling during rat limb outgrowth but not for limb initiation. Dev Dyn. 1999; 216:469–480. [PubMed: 10633866]

NIH-PA Author Manuscript

NIH-PA Author Manuscript

NIH-PA Author Manuscript

16. Dickman ED, Smith SM. Selective regulation of cardiomyocyte gene expression and cardiac morphogenesis by retinoic acid. Dev Dyn. 1996; 206:39–48. [PubMed: 9019245]
17. Kostetskii I, Jiang Y, Kostetskaia E, Yuan S, Evans T, Zile ML. Retinoid signaling required for normal heart development regulates GATA-4 in a pathway distinct from cardiomyocyte differentiation. Dev Biol. 1999; 206:206–218. [PubMed: 9986733]
18. Zile MH, Kostetskii I, Yuan S, Kostetskaia E, St. Armand TR, Chen Y, Jiang W. Retinoid signaling is required to complete the vertebrate cardiac left-right asymmetry pathway. Dev Biol. 2000; 223:323–338. [PubMed: 10882519]
19. Kim H-Y, Wolf G. Vitamin A deficiency alters genomic expression for fibronectin in liver and hepatocytes. J Biol Chem. 1987; 262:365–371. [PubMed: 3793729]
20. Ffrench-Constant C, Hynes RO. Patterns of fibronectin gene expression and splicing during cell migration in chicken embryos. Development. 1988; 104:369–382. [PubMed: 3256468]
21. Makover A, Soprano DR, Wyatt ML, Goodman DS. An in situhybridization study of the localization of retinol-binding protein and transthyretin messenger RNAs during fetal development in the rat. Differentiation. 1989; 40:17–25. [PubMed: 2744271]
22. Bavik C, Ward SJ, Chambon P. Developmental abnormalities in cultured mouse embryos deprived of retinoic acid by inhibition of yolk-sac retinol binding protein synthesis. Proc Natl Acad Sci USA. 1996; 93:3110–3114. [PubMed: 8610177]
23. Liou GI, Fei Y, Peachey NS, Matragoon S, Wei S, Blaner WS, Wang Y, Liu C, Gottesman ME, Ripps H. Early onset photoreceptor abnormalities induced by targeted disruption of the interphotoreceptor retinoid-binding protein gene. J Neurosci. 1998; 18:4511–4520. [PubMed: 9614228]
24. Smith SM, Hayes CE. Contrasting impairments in IgM and IgG responses of vitamin A-deficient mice. Proc Natl Acad Sci USA. 1987; 84:5878–5882. [PubMed: 3475707]
25. Duitsman PK, Cook LR, Tanumihardjo SA, Olson JA. Vitamin A inadequacy in socioeconomically disadvantaged pregnant Iowan women as assessed by the modified relative dose response (MRDR) test. Nutr Res. 1995; 15:1263–1276.
26. MDIS Working Paper #2: Global Prevalence of Vitamin A Deficiency. Geneva, Switzerland: World Health Organization; 1995.
27. Zerlauth G, Kim S-Y, Winner JB, Kim H-Y, Bolmer SD, Wolf G. Vitamin A deficiency and serum or plasma fibronectin in the rat and in human subjects. J Nutr. 1984; 114:1169–1172. [PubMed: 6726480]
28. Scita G, Darwiche N, Greenwald E, Rosenberg M, Politi K, De Luca LM. Retinoic acid down-regulation of fibronectin and retinoic acid receptor α proteins in NIH-3T3 cells: blocks of this response by ras transformation. J Biol Chem. 1996; 271:6502–6508. [PubMed: 8626453]
29. Mamuya WS, Brecher P. Fibronectin expression in the normal and hypertrophic rat heart. J Clin Invest. 1992; 89:392–401. [PubMed: 1531344]
30. Booz GW, Baker KM. Molecular signalling mechanisms controlling growth and function of cardiac fibroblasts. Cardiovasc Res. 1995; 30:537–543. [PubMed: 8575002]
31. Linask KK, Lash JW. A role for fibronectin in the migration of avian precardiac cells, I: dose-dependent effects of fibronectin antibody. Dev Biol. 1988; 129:315–323. [PubMed: 3417040]
32. Suzuki HR, Solursh M, Baldwin HS. Relationship between fibronectin expression during gastrulation and heart formation in the rat embryo. Dev Dyn. 1995; 204:259–277. [PubMed: 8573718]
33. Loeber CP, Runyan RB. A comparison of fibronectin, laminin, and galactosyltransferase adhesion mechanisms during embryonic cardiac mesenchymal cell migration in vitro. Dev Biol. 1990; 140:401–412. [PubMed: 2142656]
34. Ghyselinck NB, Wendling O, Messaddeq N, Dierich A, Lampron C, Decimo D, Viville S, Chambon P, Mark M. Contribution of retinoid acid receptor β isoforms to the formation of the conotruncal septum of the embryonic heart. Dev Biol. 1998; 198:303–318. [PubMed: 9659935]
35. Kubalak SW, Hutson DR, Scott KK, Shannon RA. Elevated transforming growth factor β2 enhances apoptosis and contributes to abnormal outflow tract and aortic sac development in retinoic X receptor α knockout embryos. Development. 2002; 129:733–746. [PubMed: 11830573]

NIH-PA Author Manuscript

NIH-PA Author Manuscript

NIH-PA Author Manuscript

36. Chen MM, Lam A, Abraham JA, Schreiner GF, Joly AH. CTGF expression is induced by TGF-β in cardiac fibroblasts and cardiac myocytes: a potential role in heart fibrosis. J Mol Cell Cardiol. 2000; 32:1805–1819. [PubMed: 11013125]

37. Hornberger LK, Singhroy S, Cavalle-Garrido T, Tsang W, Keeley F, Rabinovitch M. Synthesis of extracellular matrix and adhesion through β1 integrins are critical for fetal ventricular myocyte proliferation. Circ Res. 2000; 87:508–515. [PubMed: 10988244]

38. George EL, Baldwin HS, Hynes RO. Fibronectins are essential for heart and blood vessel morphogenesis but are dispensable for initial specification of precursor cells. Blood. 1997; 90:3073–3081. [PubMed: 9376588]

39. Chen T, Chang T, Kang J, Choudhary B, Makita T, Tran C, Burch J, Eid H, Sucov H. Epicardial induction of fetal cardiomyocyte proliferation via a retinoic acid-inducible trophic factor. Dev Biol. 2002; 250:198–207. [PubMed: 12297106]

40. Wagner M, Thaller C, Jessell T, Eichele G. Polarizing activity and retinoid synthesis in the floor plate of the neural tube. Nature. 1990; 345:819–822. [PubMed: 2359459]

41. Kobayashi H, Spilde TL, Bhatia AM, Buckingham RB, Hembree MJ, Prasadan K, Preutt BL, Imamura M, Gittes GK. Retinoid signaling controls mouse pancreatic exocrine lineage selection through epithelial-mesenchymal interactions. Gastroenterology. 2002; 123:1331–1340. [PubMed: 12360493]

NIH-PA Author Manuscript
NIH-PA Author Manuscript
NIH-PA Author Manuscript

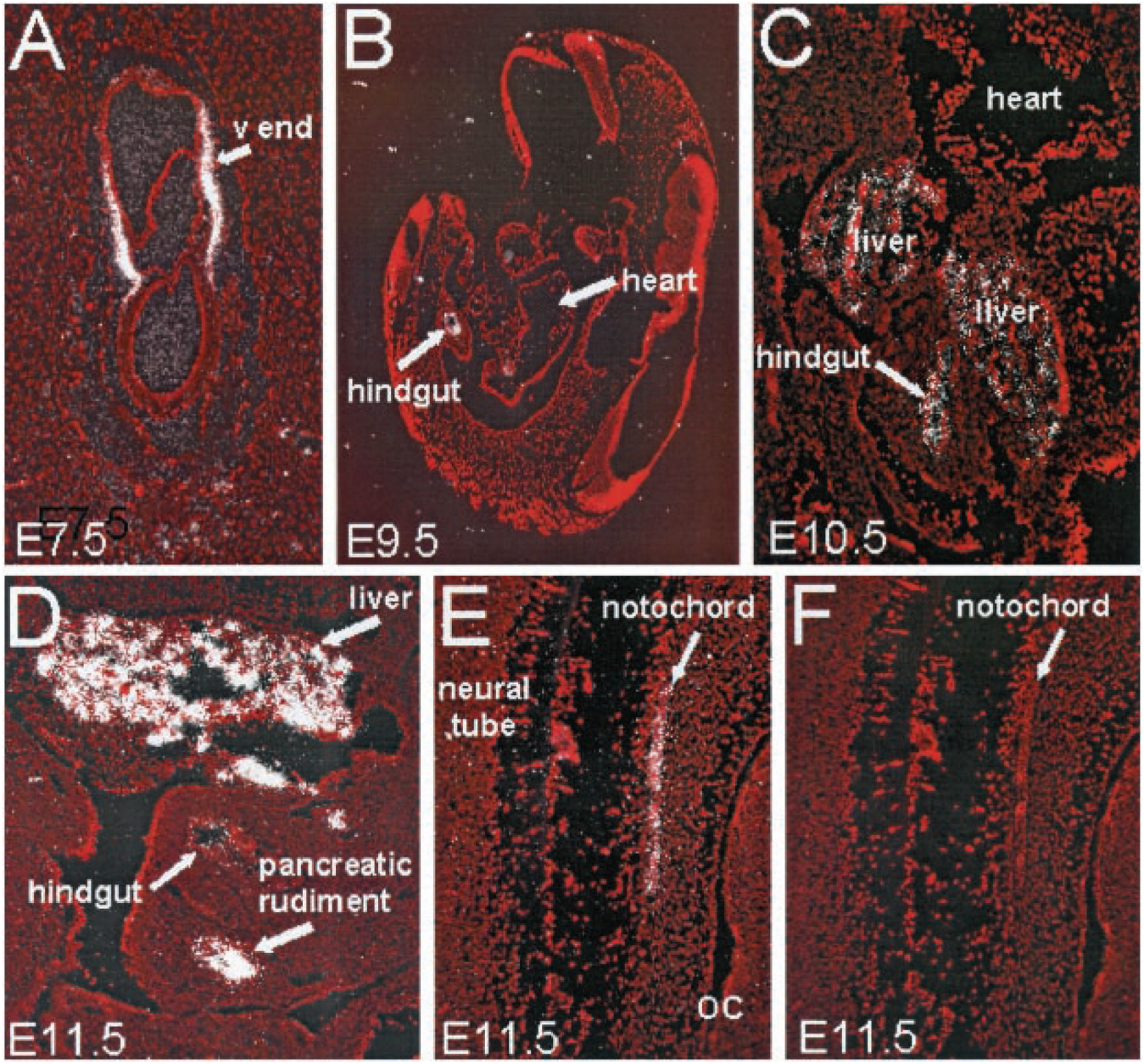

Figure 1.

In situ hybridization of RBP. A, RBP expression restricted to visceral endoderm at E7.5. B, RBP transcripts in prospective hindgut endoderm at E9.5. C, Expression in liver and gut at E10.5. D, Expression in liver and pancreatic rudiment at E11.5. E, Expression in notochord (dorsal is left, rostral at top) at E11.5. F, Same section as in panel E, with only PI-stained tissue shown. At all stages, sense riboprobe revealed no signal above background (not shown). Transcripts were detected as silver grains (white signal); nuclei were visualized with PI counterstain (red). oc indicates oral cavity; v end, visceral endoderm.

NIH-PA Author Manuscript

NIH-PA Author Manuscript

NIH-PA Author Manuscript

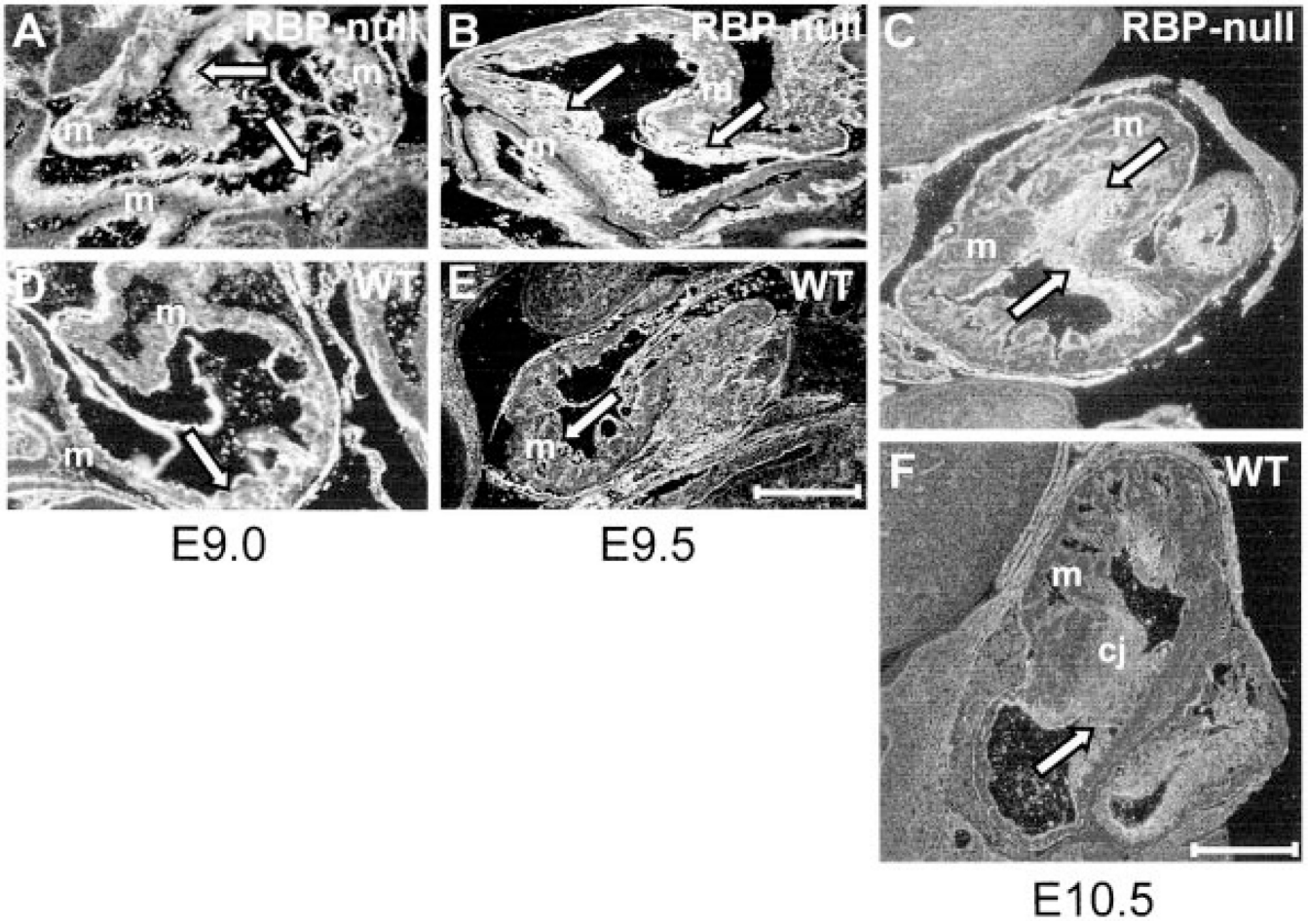

Figure 2.

RBP-null embryos exhibit increased Fn in cardiac jelly. Sections from somite stage-matched WT (D through F) and RBP-null (A through C) embryos at the indicated stages were immunostained with anti-Fn antibody (see Materials and Methods). Fn deposition in the cardiac jelly is expanded in RBP-null embryos at all stages (see arrows). Images in panels A, B, D, and E are at the same magnification. In panel E, bar=100 μm. This immunostaining pattern has been consistently observed in multiple repetitions of this determination (3 pairs of embryos at E9.0, 6 pairs at E9.5, and 4 pairs at E10.5). Images in panels C and F are at the same magnification. In panel F, bar=75 μm. m indicates myocardium; cj, cardiac jelly.

NIH-PA Author Manuscript

NIH-PA Author Manuscript

NIH-PA Author Manuscript

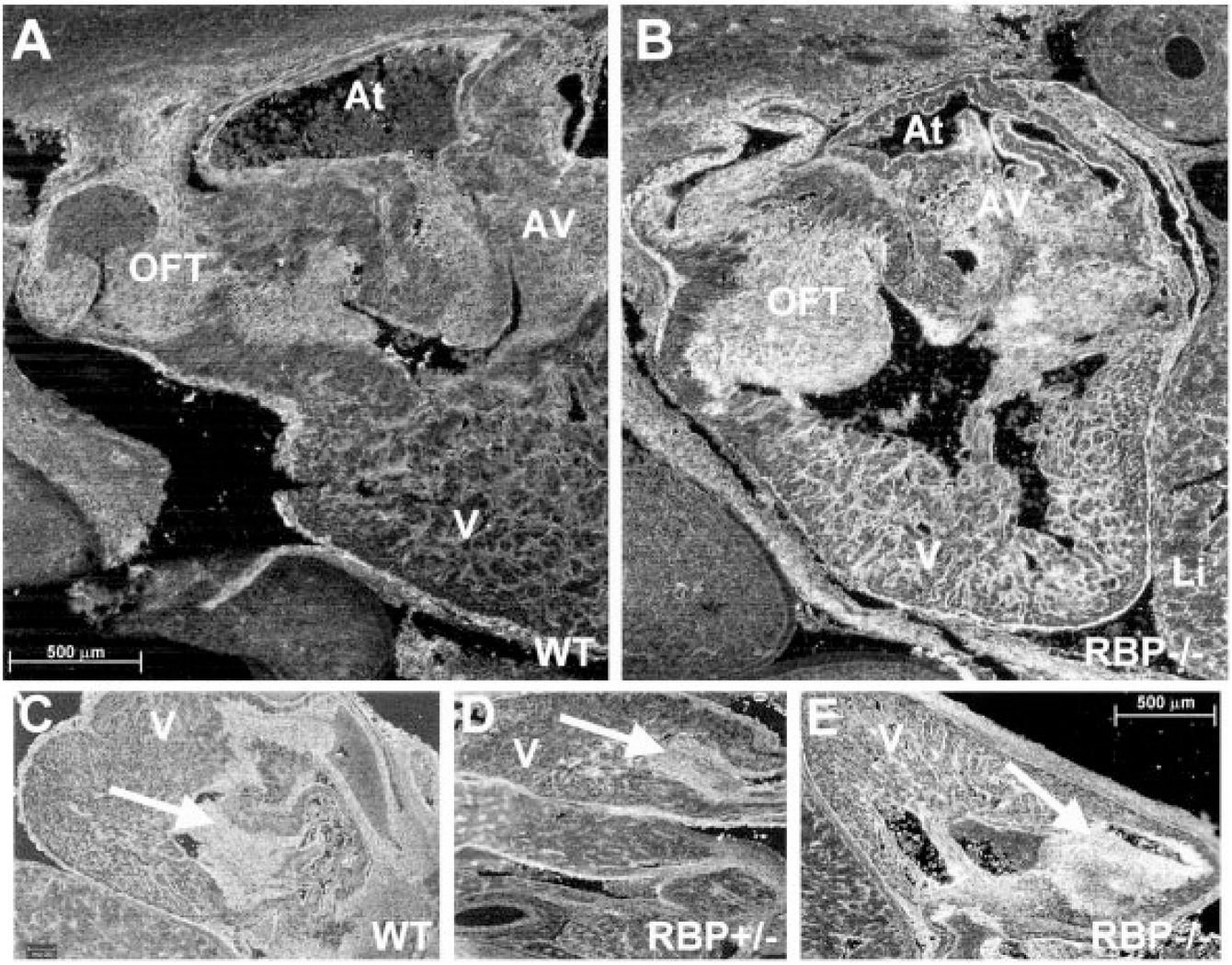

Figure 3.

Increased Fn deposition in OFT valves of RBP-null hearts at E12.5. Panels A and B are Fn-immunostained sections from WT and RBP-null (RBP−/−) hearts, respectively, of embryos from separate litters. Panels C, D, and E show sections from WT, heterozygous (RBP+/−), and null (RBP−/−) hearts, respectively, from littermates. Note the increased Fn signal in OFT and AV valves (C through E, arrows) in RBP-null (B and E) but not WT (A and C) or heterozygous (D) hearts. This pattern was observed in 4 repetitions of this determination. Panels A and B are at the same magnification (A, size bar); panels C through E are at the same magnification (E, size bar). At indicates atrium; AV, atrioventricular canal; V, ventricle; and Li, liver.

NIH-PA Author Manuscript

NIH-PA Author Manuscript

NIH-PA Author Manuscript

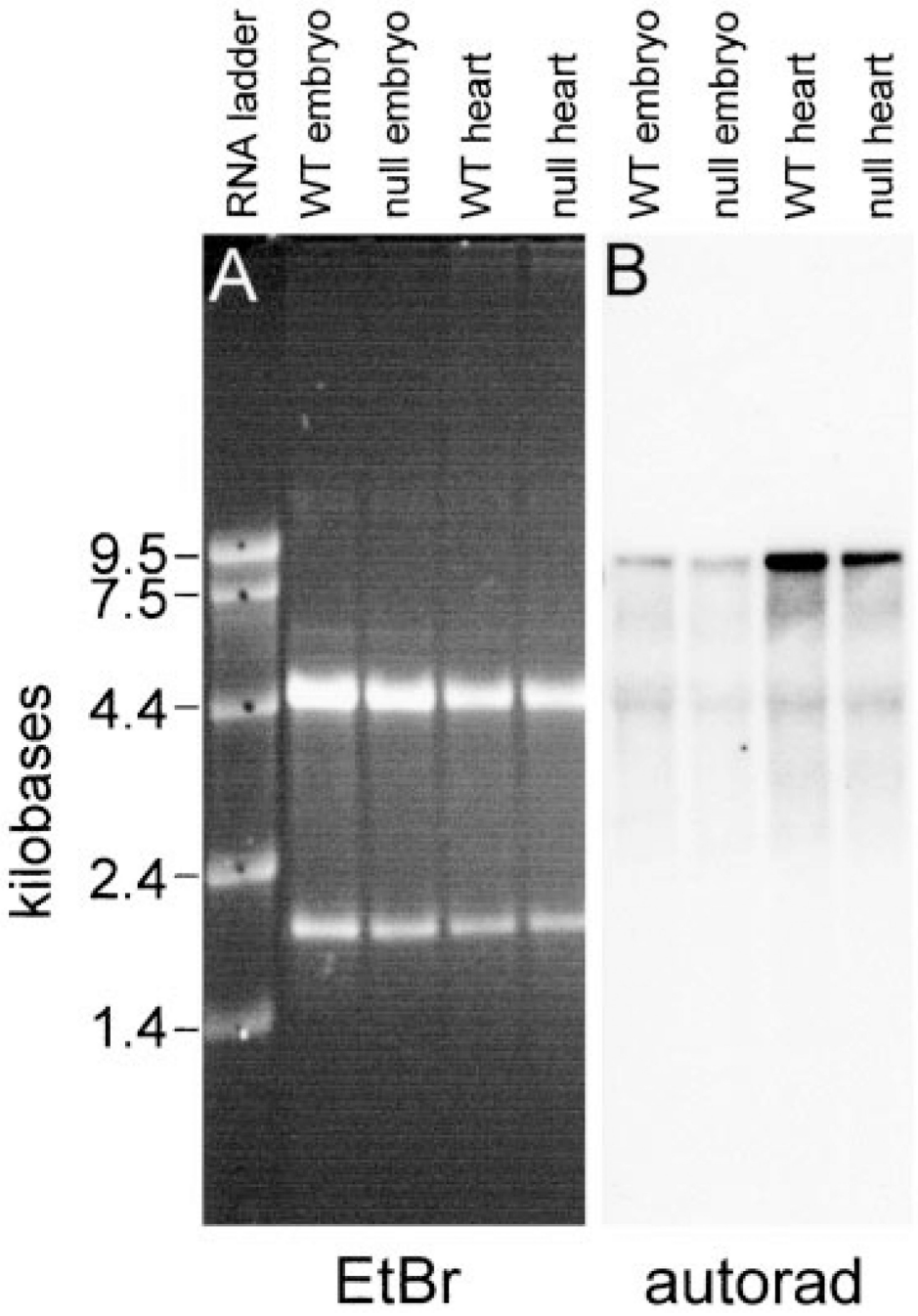

Figure 4.

Northern hybridization of Fn transcripts. Total RNA (1 μg) from whole embryos or isolated hearts of WT and RBP-null embryos was separated by agarose/formaldehyde electrophoresis (A), and the blot was hybridized with antisense riboprobe to Fn mRNA (B). Fn transcript levels in WT and RBP-null tissues were not appreciably different; repetition of this determination did not reveal the subtle increase in Fn transcripts noted in WT heart RNA. EtBr indicates ethidium bromide; autorad, autoradiography.

NIH-PA Author Manuscript
NIH-PA Author Manuscript
NIH-PA Author Manuscript

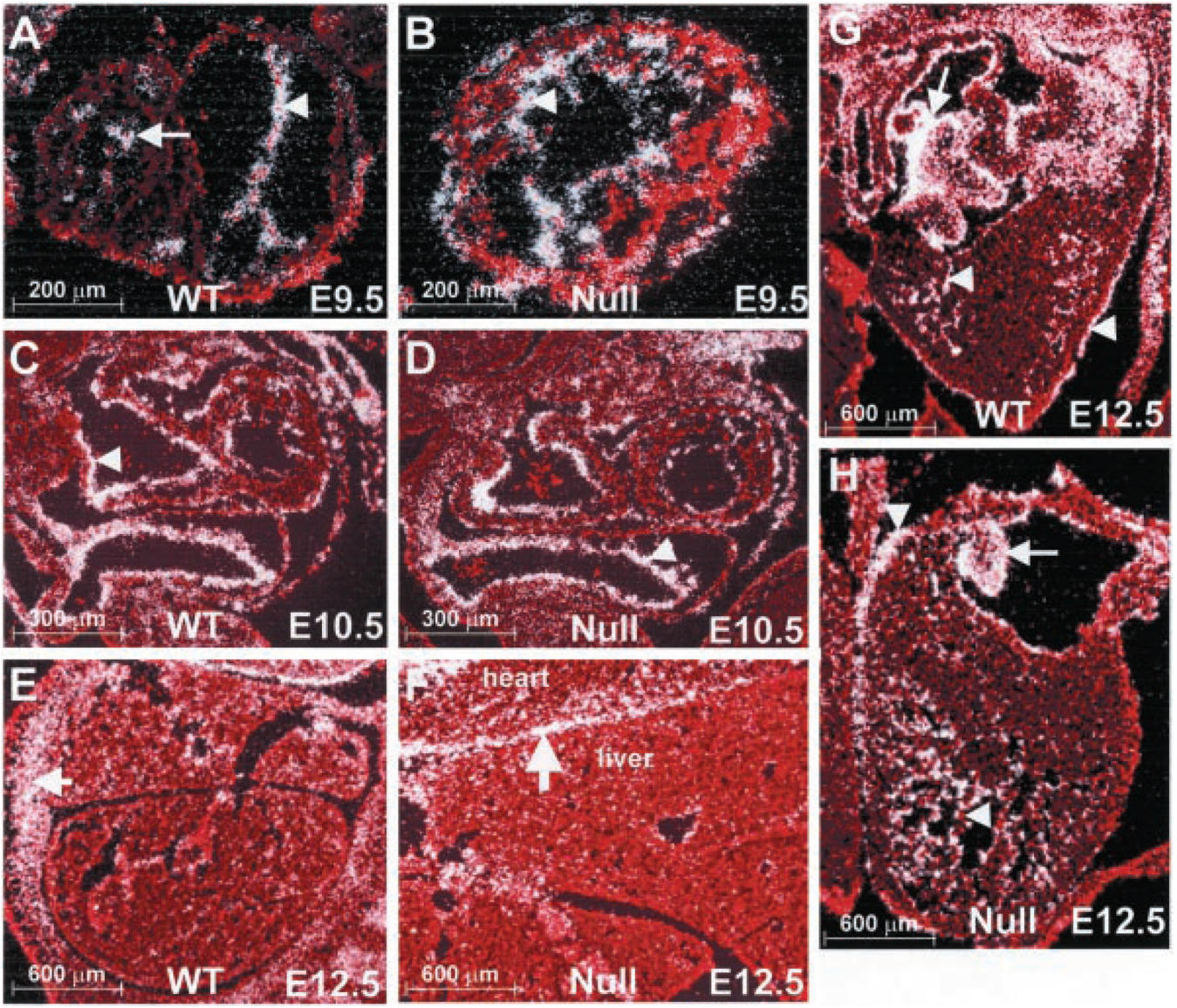

Figure 5.

In situ hybridization of Fn transcripts. Sections were hybridized with the same antisense riboprobe used for Figure 4. At E9.5 (A and B), Fn mRNA was detected in endocardiocytes (arrowheads), with lower expression in scattered cells within the myocardium (A, arrow). At E10.5 (C and D), transcripts were in endocardial cells (arrowheads) lining ventricles, atria, and OFT, as well as in the epicardium (not shown). By E12.5 (G and H), most signal was in the endocardial cushions (arrows) and endocardial and epicardial linings (arrowheads). Fn was absent from cardiomyocytes at E10.5 and E12.5. No difference in Fn expression was seen between WT and RBP-null hearts at any stage or in livers at E12.5 (E and F). Repetition of these determinations in identically staged embryos revealed the same hybridization pattern. Arrow in panel E shows Fn-expressing mesoderm in the anterior body wall; arrow in panel F points to the septum transversum. White silver grains indicate Fn signal; red is PI-stained nuclei.

NIH-PA Author Manuscript
NIH-PA Author Manuscript
NIH-PA Author Manuscript

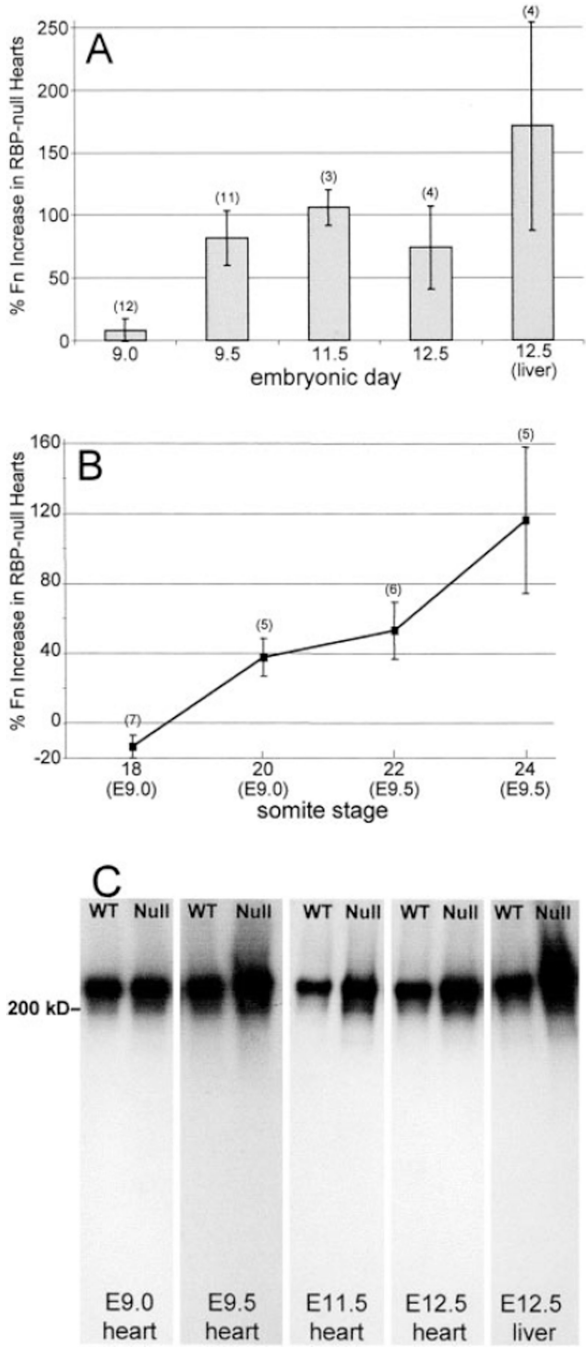

Figure 6.

Western blot analysis of Fn protein. Samples containing identical fractions of protein from WT and RBP-null hearts were Western-blotted. Panel A shows cumulative data from WT and RBP-null sample pairs (number of sample pairs is shown in parentheses on graph), revealing Fn increases in the latter between E9.0 and E12.5. Panel B shows that when data from sample pairs at E9.0 through E9.5 are grouped according to somite stage rather than postcoital days, the increase in Fn expression in RBP-null hearts is essentially linear with time. Panel C shows representative Western blots at the indicated stages that were used to construct the data in panels A and B. Parallel lanes at each stage were loaded with equal fractions of total protein from WT or RBP-null heart or liver. At E9.0, each aliquot was

equivalent to 1 heart; at E9.5, 1/2 heart; at E11.5, 1/25 heart; at E12.5, 1/50 heart; and at E12.5, 1/100 liver.

NIH-PA Author Manuscript
NIH-PA Author Manuscript
NIH-PA Author Manuscript

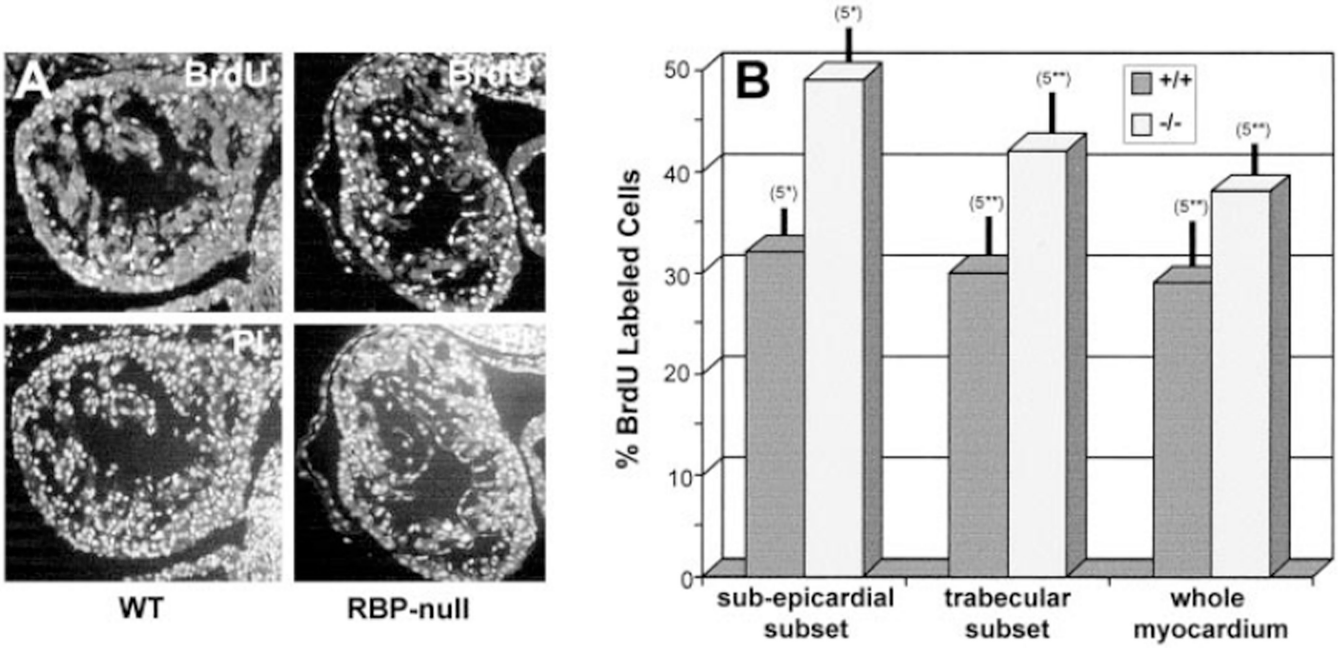

Figure 7.

Increased cell proliferation in RBP-null myocytes. Cell proliferation in E10.5 hearts was monitored by BrdU incorporation. After embedding and sectioning were performed, dividing cells were detected by anti-BrdU immunohistochemistry, followed by PI staining to mark all nuclei. Sections from WT and RBP-null hearts are shown in panel A. Panel B presents the percentage of BrdU incorporation in 3 subsets of myocardial cells. Total numbers of nuclei evaluated to calculate each average, which was obtained from 5 pairs of hearts, were ≈9000 for the “whole myocardium” subset, 3000 for the “trabecular” subset, and 2000 for the “subepicardial” subset. This revealed statistically significant increases in percentage of BrdU-labeled nuclei in all areas of RBP-null embryonic hearts. Vertical bars indicate ±SEM. Significance between means was determined by Student *t* test: ** $P<0.04$ and * $P=0.004$.

NIH-PA Author Manuscript NIH-PA Author Manuscript NIH-PA Author Manuscript

NIH-PA Author Manuscript
NIH-PA Author Manuscript
NIH-PA Author Manuscript

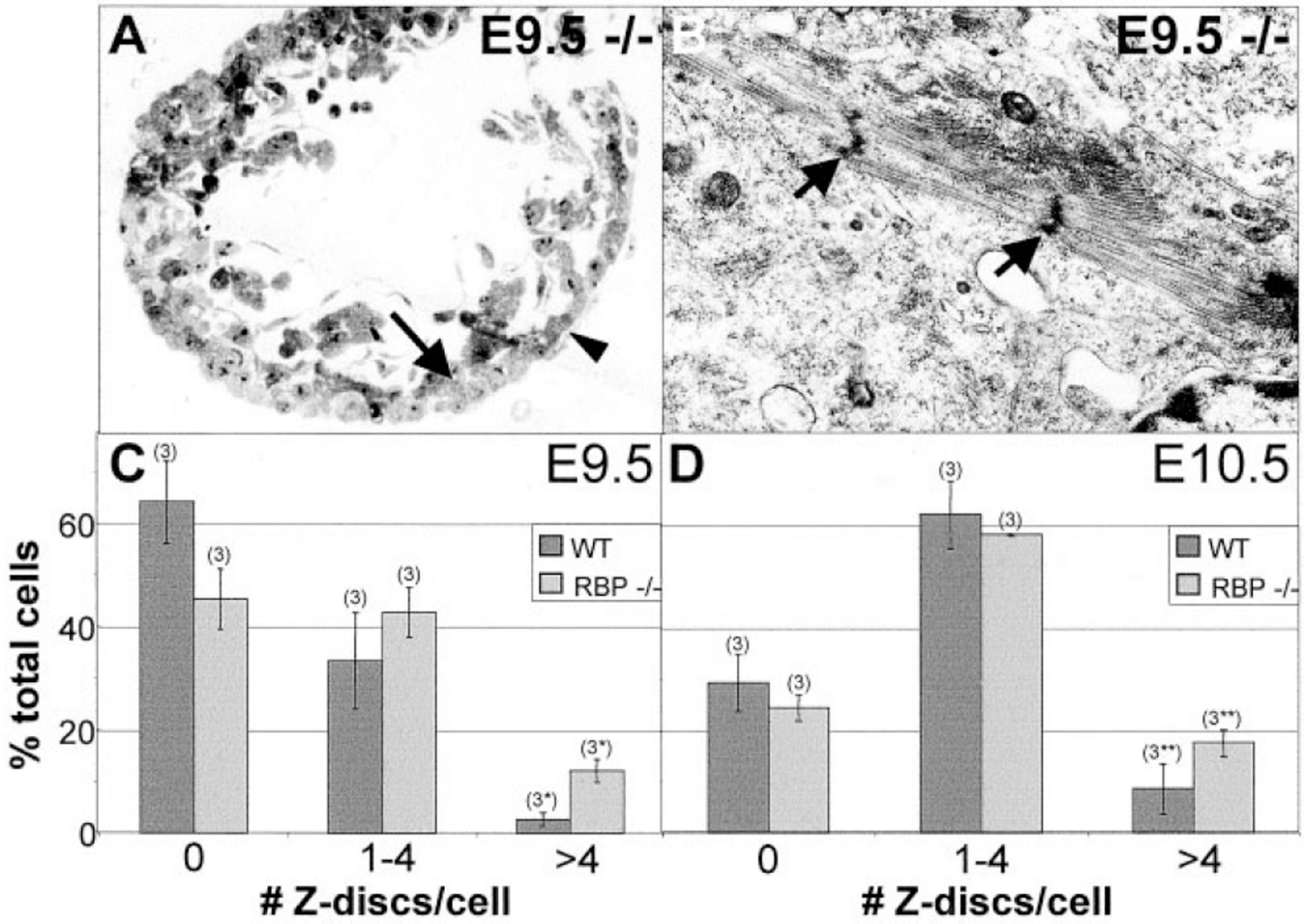

Figure 8.

Subepicardial myocytes are precociously differentiated in RBP−/− hearts. Subepicardial myocytes in 3 pairs of E9.5 and E10.5 WT and RBP−/− hearts were ultrastructurally evaluated for numbers of Z disks, a structure indicating sarcomere differentiation. Panel A is a light micrograph of an E9.5 RBP−/− heart showing the subepicardial myocyte layer (arrow) and the investing layer of epicardial cells (arrowhead). Panel B is an electron micrographic image of a myocyte in the subepicardial layer; arrows point to Z disks. Panels C and D show quantitative data indicating the percentage of myocytes in the subepicardial region of WT and RBP−/− hearts that contain 0, 1 to 4, or >4 Z disks per cell. Vertical bars indicate ±SEM; levels of statistical significance were determined by Student *t* test: **P*<0.01 and ***P*<0.09.